Absorption ability and kinetics of a liquid electrolyte in PVDF–HFP copolymer containing or not SiO$_2$

M. Caillon-Caravanier, B. Claude-Montigny, D. Lemordant, G. Bosser[*]

Laboratoire de Physico-Chimie des Interfaces et des Milieux Réactionnels (PIMIR), EA 2098, U.F.R des Sciences et Techniques, Parc de Grandmont, 37200 Tours, France

Abstract

Gel polymer electrolytes have been prepared from PVDF–HFP copolymer with various silica contents incorporating Gamma valerolactone (VL) or VL/EC (80/20 in mole) (EC: ethylene carbonate) solutions of lithium bis(trifluoromethane sulfone) imide (LiTFSI). The influence of temperature, salt content and silica addition on the kinetics of absorption and wettability of the copolymer has been investigated. An empirical model, taking into account gel swelling during the absorption allows us to relate, at constant temperature, the wetting time and the volumetric fraction of trapped electrolyte, which is a critical factor for ionic conductivity of the gel. Increasing the silica content in the dry copolymer increases the porosity and consequently the rate of absorption and thus the amount of incorporated liquid phase at saturation. To a lower extent, an increase in the temperature of absorption has the same effects. The prepared gels have good mechanicals properties and conductivities. As an example, a gel of composition:

PVDF−HFP/SiO$_2$/VL/EC/LiTFSI of molar percentages 36/6.7/42/10.5/4.8 exhibits a conductivity of 2.9 mS cm^{-1} at 293 K.

© 2002 Elsevier Science B.V. All rights reserved.

Keywords: PVDF–HFP copolymer; VL/EC/LiTFSI plasticizer; Wettability; Absorption kinetics

1. Introduction

Previous works have revealed the various appealing properties of PVDF–HFP copolymer as host for liquid electrolytes for applications in rechargeable lithium batteries [1–4]. In a recent article [5], J.Y. Song et al. have determined an average pore diameter of 16.4 nm and a Brunauer–Emmett–Teller surface area of 128 m^2 g^{-1} for PVDF–HFP copolymer (Kynar FLEX 2801, from Elf Atochem). The ionic conductivity of these porous membranes is due to the conductivity of the liquid electrolyte embedded in the pores [4]. As a consequence, it is greatly affected by the porosity and the wetting properties of the membrane [6].

It has been shown that adding silica, in the composition range: 2 < wt.% SiO$_2$ < 10, increases the wettability of the dry copolymer and, therefore, the ionic conductivity [3]. Higher silica contents lead to a decrease in conductivity because of Li$^+$ fixation, clearly evidenced by NMR spectroscopy [7]. For that reason, in this work, the final contents in silica have been fixed to 0, 4 and 8 wt.%.

The conductivity of gamma valerolactone (VL)–lithium bis(trifluoromethanesulfone) imide (LiTFSI) solutions is, at the present time, studied in our laboratory. The solvent presents a high solvating power toward lithium cation and a good chemical stability relative to lithium metal [8]. Furthermore, low melting and high boiling temperatures (−31 and 207 °C, respectively), relatively high permittivity and moderate viscosity ($\varepsilon_r = 32$ and $\eta = 1.89$ mPa s at 25 °C) make this solvent a promising candidate as a component of gel electrolytes. The addition of ethylene carbonate (EC) improves the stability of the passivation layer at the carbon anode-electrolyte interface [8,9], but it raises the melting point of the solution and limits the operating temperature range. So the molar percentage of EC has been limited to 20% for this study. The anodic electrochemical stability of the VL/EC(80/20)–LiTFSI 1 M electrolyte was determined, relatively to a reference lithium electrode, on platinum (Pt), Nickel (Ni) and stainless steel (SS), and characterized by the potential at which the current onset occurs: 5.7 V on Pt, 4.8 V on Ni and 4.4 V on SS.

Unfortunately, the practical use of LiTFSI has not materialized, due to its severe corrosion of Al, which is commonly used as a cathode current collector, above 3.6 V

---

* Corresponding author.
E-mail address: bosser@univ-tours.fr (G. Bosser).

Nomenclature

$C_{l,0} = C_{l,sat}$ (g l^{-1})	weight concentration of the wetting liquid phase in the saturated polymer
J_t (g cm^{-2} s^{-1})	Massic flux of the diffusing liquid threw the copolymer–liquid electrolyte interface at time t
k (g cm^{-2} s^{-1})	kinetic constant relative to the absorbed weight of liquid phase
$m_{l,0}$ (g)	absorbed weight of the liquid phase in the fast initial stage of the superficial wetting of the copolymer
$m_{0,P}$ (g)	initial weight of the dry copolymer
$m_{l,t}$, $m_{l,sat}$ (g)	absorbed weight of the liquid phase at time t and at saturation
S_0; S_t; S_{sat} (cm^2)	surface area of the sample at initial time, time t and at saturation
W_{ab}	weight percentage of absorption of the liquid phase relative to the initial weight of the dry copolymer
$V_{0,P}$, V_t; V_{sat} (cm^3)	sample volume at initial time, time t and at saturation
$V_{l,sat}$ (cm^3)	volume of the liquid phase in the saturated gel
V_{ab}	volumetric percentage of absorption of the liquid phase relative to the initial volume of the dry copolymer
Greek letters	
α_t^{ab}	advancement of the liquid phase absorption into the copolymer at time t
$\Phi_{l,sat}$	volumetric fraction of the liquid phase into the gel
σ_G, $\sigma_{l,G}$ (S cm^{-1})	conductivity of the gel and of the liquid phase in the gel respectively

versus Li/Li$^+$ [9,10], and LiPF$_6$ is, for this reason, preferred to LiTFSI in rechargeable batteries.

Nevertheless, in the same conditions, LiTFSI and LiPF$_6$ based electrolytes have comparable conductivities and, furthermore, LiTFSI has better chemical and thermal stability and safety characteristics [11,12].

So, the main aim of this work being to precise quantitatively the influence of salt content in the liquid phase, of the silica content in the dry polymer, and of the temperature on the rate of the wetting process and final composition of the gel electrolyte, we used the LiTFSI salt. In a near future, the same study, on commercialy available liquid electrolytes such as "LP30 Selectipur®" (from MERCK: EC/DMC (50/50) in wt.% —LiPF$_6$ 1 M), will be undertaken.

2. Experimental

2.1. Materials

Copolymer PVDF–HFP(92/8) "SOLEF" and silica (AEROSIL R 972) were provided respectively by SOLVAY and DEGUSSA–HULS. Silica was dried under vacuum at 260 °C for 24 h before use. Dibutyl phatalate (DBP, 99%), the initial plasticizer, and EC (98%) from ALDRICH were used as received. Gamma VL (99%), also from ALDRICH, was dried over molecular sieves and stored under argon. Lithium bis(trifluoromethane sulfone) imide (LiTFSI) from 3 M was dried at 140 °C under vacuum for 24 h and then, stored under argon in a dessicator. Diethyl ether and acetone, from COFRALAB were dried by distillation and stored under argon.

2.2. Preparation of microporous polymeric membranes

PVDF–HFP copolymer was dissolved first in acetone at 40 °C, then DBP was added and finally silica. The mixture has been homogeneized under argon by vigoreous stirring. The resulting solution was cast on aluminium plates and acetone was allowed to evaporate slowly. Next, the membrane was weighed, immersed in diethyl ether for about 24 hours under continuous stirring in order to extract DBP and, after drying at 60 °C under vacuum, weighed again to confirm the total extraction of DBP.

2.3. Absorption kinetics study

The dry copolymer was punched in circular pieces whose diameter and thickness were measured with an electronic calliper square. After being accurately weighed, the samples were immersed in the thermostated liquid electrolyte. At regular intervals, the samples were taken out, pressed lightly between two sheets of clean filter paper and weighed. For a given membrane and a fixed electrolyte composition, experiments were run in triplicate or more.

2.4. Determination of intermediate and final compositions

The sizes, measured at room temperature, and weight of the samples, allowed us to determine the weight of liquid electrolyte absorbed by the membrane with time and, for some samples, the evolution of surface area with time. Assuming no compression of the liquid phase in the gel, the volumetric fraction of liquid electrolyte at saturation was calculated using the relative densities measured by the pycnometric method.

2.5. Conductivity

Conductivity of the gels was obtained by complex impedancemetry using a Solartron ST 1260 impedance/gain phase analyser in the frequency range 1 Hz to 10 MHz.

The samples were sandwiched between two stainless steel electrodes in homemade thermostated cells. Liquid electrolytes conductivities were determined using a Crison GLP 31 conductimeter operating at variable frequency and a conductivity cell Crison S2-92 with platinum electrodes covered by black platinum (cell constant: $1\ cm^{-1}$). All solutions were prepared into a 50-cm^3 double wall thermostatable cell, under argon atmosphere.

2.6. Raman spectroscopy

FT Raman spectra were recorded on a Brucker RFS 1000 spectrometer with a near-infrared YAG laser source at 1064 nm. The laser power on the sample is 100 mW with a light spot of 0.1 mm diameter. The scattered light is collected in the direction of $180°$ to the incident light. Each Raman spectrum was the result of one hundred scans. FT Raman spectra with a wavenumber resolution of $2\ cm^{-1}$ were recorded at ambient temperature. An OS/2 operating system was used both to collect and to process the data.

3. Results and discussion

3.1. Homogeneity of the absorption

Prior to examine kinetic results and absorption abilities of the copolymers, we have to verify the homogeneity of absorption process. The initial composition of the liquid phase is chosen to provide the highest conductibility as possible. It is necessary to verify that the composition of the absorbed liquid phase is identical to the initial liquid electrolyte. Two methods have been employed for this purpose. First, the conductivity of the liquid phase used for copolymer wetting is measured before and after absorption of a significant fraction of initial liquid volume. We verify that conductivity is the same, in the interval of apparatus accuracy, before and after wetting as expected for an homogeneous absorption. Secondly, the intensity of the Raman line at $741\ cm^{-1}$ which was assigned to the $\delta_s(CF_3)$ vibration characteristic of $TFSI^-$ anion [13,14], is measured in VL/LiTFSI solutions and in gels. In liquid phases the integrated intensity of $\delta_s(CF_3)$ mode is proportional to the molar percentage of the salt (see Fig. 1). If there is no strong interaction between the anion and the polymer network in the gel, the intensity of this Raman line must exhibit the same behaviour. We can see in Fig. 1, the integrated intensities of $741\ cm^{-1}$ Raman line in relation with salt molar percentages in gels: 1.2, 2.4, 4.6 and 6.3%, resulting from saturation of the PVDF–HFP copolymer by VL/LiTFSI solutions with salt molar percentages: 2, 4, 6, and 8%.The experimental intensities are in close correlation with the expected one represented by the drawn line. All these results confirm the homogeneity of the liquid electrolyte absorption by the copolymer.
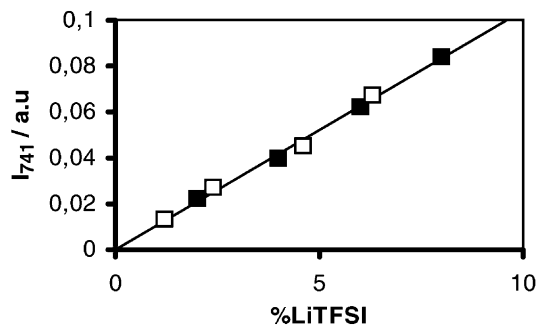

Fig. 1. Integrated intensities of $\delta_s(CF_3)$ vibration Raman bands at $741\ cm^{-1}$ for VL/LiTFSI solutions (■) and PVDF–HFP/VL/LiTFSI gels (□). The drawn line is linear regression analysis of I_{741} for VL/LiTFSI solutions which gives: $I_{741} = 0.0104$. %LiTFSI in arbitrary units.

3.2. Amount of liquid electrolyte absorbed with time

We will examine first the theoretical models used to describe the absorption kinetic, then the influence of liquid phase, copolymer composition and temperature on the rate of absorption. In the last section, we will compare the absorption capacity in relation with the same factors. The symbols used and their meaning are reported in the nomenclature section.

3.2.1. Diffusion model

The advancement of liquid electrolyte absorption in the PVDF–HFP membrane (α_t^{ab}) is defined as the ratio of the adsorbed weight at time t ($m_{l,t}$) to the adsorbed weight at saturation ($m_{l,sat}$):

$$\alpha_t^{ab} = \frac{m_{l,t}}{m_{l,sat}} \tag{1}$$

For $0 < \alpha_t^{ab} < 0.6$, the kinetic of absorption is well described by a diffusion model based on Fick's second law [15,16]. This model implies the hypothesis, supported by experimental evidence that, in the first stage of the process, a rapid wetting of the surface of the copolymer occurs. This rapid wetting corresponds to the saturation of the surface pores by the liquid phase leading to a thin layer where the weight concentration $C_{l,0}$ of liquid phase is equal to its final value $C_{l,sat}$:

$$C_{l,0} = C_{l,sat} = \frac{m_{l,sat}}{V_{sat}} \tag{2}$$

Starting from this saturated layer, the solution diffuses into the polymer. The massic flux of diffusing liquid, J_t, is given by [15,16]:

$$J_t = \frac{1}{S_t}\left(\frac{dm_{l,t}}{dt}\right) = C_{l,sat}D^{1/2}\pi^{1/2}t^{1/2} = Kt^{-1/2} \tag{3}$$

where D is the average diffusion coefficient of particles and S_t is the cross sectional area of the sample at time t.

By integrating Eq. (3) relatively to the time, the weight of liquid phase absorbed at time t is obtained:

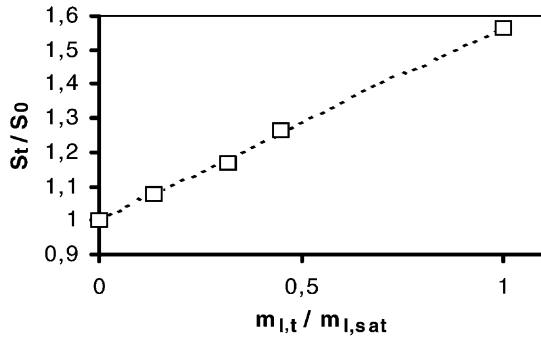$$m_{l,t} = \int_0^t S_t J_t\ dt \tag{4}$$

Fig. 2. Evolution of the surface area of PVDF–HFP copolymer wetted by a VL/LiTFSI(92/8) solution at 20 °C (dotted line is linear regression).

In this particular case, it has been taken into account the increasing surface area of the copolymer solution interface produced by gel swelling. In order to determine the variation of S_t with time, samples sizes were measured for increasing times of absorption. In Fig. 2, the normalized area of the sample S_t/S_0 has been plotted against the advancement α_t^{ab}. As, within experimental error, S_t/S_0 increases lineary with α_t^{ab}, the variation of S_t with time is given by:

$$S_t = S_0 + \alpha_t^{ab}(S_{sat} - S_0) \tag{5}$$

or

$$S_t = S_0 + Bm_{1,t}$$

with

$$B = \frac{S_{sat} - S_0}{m_{1,sat}}$$

Combining Eqs. (3) and (5); we obtain:

$$\frac{dm_{1,t}}{dt} = (S_0 + Bm_{1,t})Kt^{-1/2} \tag{6}$$

After integration, ones obtain:

$$\frac{1}{B}\ln\left[1 + \left(\frac{B}{S_0}\right)m_{1,t}\right] = 2Kt^{1/2} + \text{cte}$$

Using the initial condition: $m_{l,t} = m_{l,0}$ at $t = 0$, leads to:

$$\ln\left[1 + \left(\frac{B}{S_0}\right)m_{1,t}\right] = \ln\left[1 + \left(\frac{B}{S_0}\right)m_{1,0}\right] + 2KBt^{1/2} \tag{7}$$

In Fig. 3, the variations of $\ln\left[1 + (B/S_0)m_{1,t}\right]$ has been plotted against $t^{1/2}$. The plot is linear unless the saturation is approached. A linear regression analysis operated at short times ($t < 45'$) allow us to determine the slope of the correlation and hence, the diffusion coefficient from the relation:

$$D = 4\pi\left[\frac{2BKV_{1,sat}}{S_{sat} - S_0}\right]^2 \tag{8}$$

For the sample studied:

$m_{0,P} = 0.1011\,\text{g};\quad m_{1,sat} = 0.2806\,\text{g};\quad V_{0,P} = 0.145\,\text{cm}^3;$
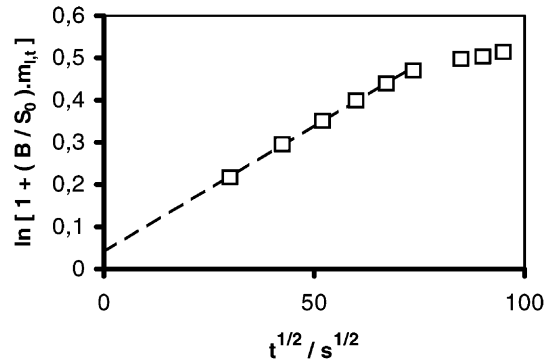$V_{sat} = 0.312\,\text{cm}^3.$

Fig. 3. Exploitation of the diffusion model for absorption of a liquid phase VL/LiTFSI(92/8) by the copolymer PVDF–HFP/SiO$_2$(73/27) at 20 °C; ($\square$): calculated values of $\ln\left[1 + (B/S_0)m_{1,t}\right]$; with $B = (S_{sat} - S_0) \times m_{1,sat}^{-1}$. Linear regression analysis (dotted line) of the first five points: $\ln[1 + (B/S_0)m_{1,t}] = 0.0393 + 5.994.10^{-3}\,t^{1/2}$, $r^2 = 1.000$.

$S_0 = 2.891\,\text{cm}^2;\quad S_{sat} = 4.925\,\text{cm}^2$:
$S_0 - S_{sat} = 2.034\,\text{cm}^2.$

Diffusion coefficient from Eq. (8): $D = 1.1 \times 10^{-5}\,\text{cm}^2\,\text{s}^{-1}$.

3.2.2. Modified model

In order to describe the whole absorption process, it is assumed that the rate of absorption is proportional to both the solution—copolymer interface area and the fraction of empty pores in the material. At time t, the fraction of empty pores is defined by: $1 - (m_{1,t}/m_{1,sat})$ These assumptions, considering Eq. (5), leads to:

$$\frac{dm_{1,t}}{dt} = k(S_0 + Bm_{1,t})\left[1 - \left(\frac{m_{1,t}}{m_{1,sat}}\right)\right] \tag{9}$$

where k is a kinetic constant.

Integration of Eq. (9) with respect to initial conditions leads to the following expression:

$$\ln\left[\frac{a + m_{1,t}}{b + cm_{1,t}}\right] = Y_{2,0} + k_{exp}t \tag{10}$$

where $Y_{2,0}$ is an integration constant given by: $Y_{2,0} = \ln[(a+m_{1,0})/(b+cm_{1,0})]$ with

$$a = \frac{S_0 m_{1,sat}}{S_{sat} - S_0}, \quad b = \frac{S_{sat} - S_0}{m_{1,sat}}, \quad c = \frac{-(S_{sat} - S_0)}{m_{1,sat}^2}$$

and

$$k_{exp} = \frac{kS_{sat}}{m_{1,sat}}$$

The absorbed weight at time t can be deduced from Eq. (10):

$$m_{1,t} = \frac{[b\exp(Y_{2,0})\exp(k_{exp}t)] - a}{1 - [c\exp(Y_{2,0})\exp(k_{exp}t)]} \tag{11}$$

Examination of Fig. 4 shows that the graph $\ln[(a+m_{1,t})/(b+cm_{1,t})] = f(t)$ is linear.
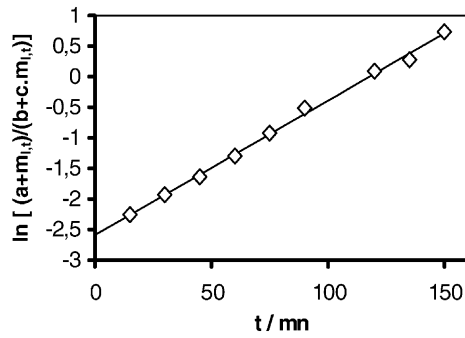
Fig. 4. Exploitation of the modified model for the absorption of a liquid phase VL/LiTFSI(98/2) by the copolymer PVDF–HFP/SiO$_2$ (73/27) at 20 °C. ($\diamond$); calculated values of $\ln[(a+m_{1,t})/(b+cm_{1,t})]$; full line: linear regression which gives: $\ln[(a + m_{1,t})/(b + cm_{1,t})] = -2.592 + 0.0220\,t$, $r^2 = 0.998$.

The sample studied is the same as in Fig. 3, so:

$$a = 0.3988\,\text{g}; \quad b = 7.2488\,\text{cm}^2\,\text{g}^{-1}; \quad c = -25.833\,\text{cm}^2\,\text{g}^{-2}.$$

Regression analysis give both $m_{1,0}$ and $k_{\exp}$ values:

$$m_{1,0} = 0.049\,\text{g} \quad \text{and} \quad k_{\exp} = 2.20 \times 10^{-2}\,\text{mn}^{-1}$$

gives : $k = 2.1 \times 10^{-5}\,\text{g}\,\text{cm}^{-2}\,\text{s}^{-1}$.

In Fig. 5, the variations of the weight of absorbed liquid in two samples versus time at −2.5 and 30 °C. Geometric and kinetic parameters for the simulations are:

$$-2.5\,°\text{C}: \ S_0 = 3.01\,\text{cm}^2; \quad V_{0,P} = 0.128\,\text{cm}^3;$$

$$S_{\text{sat}} = 4.30\,\text{cm}^2; \quad V_{\text{sat}} = 0.262\,\text{cm}^3; \quad m_{1,0} = 0.051\,\text{g};$$

$$m_{1,\text{sat}} = 0.245\,\text{g}; \quad k_{\exp} = 1.92 \times 10^{-2}\,\text{mn}^{-1}.$$

$$30.0\,°\text{C}: \ S_0 = 7.32\,\text{cm}^2; \quad V_{0,P} = 0.306\,\text{cm}^3;$$

$$S_{\text{sat}} = 10.74\,\text{cm}^2; \quad V_{\text{sat}} = 0.684\,\text{cm}^3; \quad m_{1,0} = 0.075\,\text{g};$$

$$m_{1,\text{sat}} = 0.628\,\text{g}; \quad k_{\exp} = 3.53 \times 10^{-2}\,\text{mn}^{-1}.$$

As the curves, calculated by Eq. (11) fit the experimental points, it can be concluded that the modified model is able to describe satisfactorily the whole process of absorption.
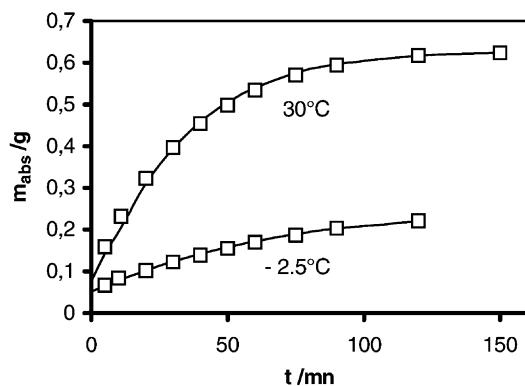

Fig. 5. Experimental (markers) and simulated (drawn lines) evolutions of the absorbed weight of a liquid phase VL/LiTFSI(88/12) by the copolymer PVDF–HFP/SiO$_2$ (73/27) at −2.5 and 30 °C.

Table 1
Diffusion coefficients and kinetic constants at various temperatures for the absorption of VL/TFSI solutions in the PVDF–HFP/SiO$_2$ copolymer

θ (°C)	%TFSI	0	1	2	4	8	12
0	$10^5 \times k^a$	2.36	1.82[c]				2.06
	$10^5 \times D^b$	0.75	0.68[c]				0.55
10	$10^5 \times k^a$	3.02	2.58				3.12
	$10^5 \times D^b$	1.09	1.04				0.84
20	$10^5 \times k^a$	3.69	3.02	2.23	2.54	3.72	4.23
	$10^5 \times D^b$	1.49	1.45	1.12	1.11	1.40	1.33
30	$10^5 \times k^a$	4.83	3.50				5.99
	$10^5 \times D^b$	1.94	1.73				1.65

[a] In g cm^{-2} s^{-1}.
[b] In cm^2 s^{-1}.
[c] Measured at −2.5 °C.

3.3. Kinetics results

3.3.1. Influence of salt content in the liquid phase and of the temperature

The influence of salt content in the liquid phase and of the temperature on the rate of absorption are studied for an initial molar percentage composition of copolymer PVDF–HFP/SiO$_2$ (73/27) and for VL/LiTFSI solutions where the molar fraction of salt, X_{LiTFSI} is between 0 and 0.12, in the temperature range $0 < \theta(°\text{C}) < 30$. The kinetics results, k and D values, are reported in Table 1 for different temperatures and contents in salt. The following conclusions can be drawn.

(i) As expected, kinetic absorption constants and diffusion coefficients are closely related.

(ii) Increasing the salt content relatively to the pure solvent first reduces the rate of absorption and, for $X_{\text{LiTFSI}} > 0.04$, enhances the rate of the process. This behaviour can be explained by taking into account two competitive effects: solvated ions are much larger entities than solvent molecules and steric hindrance for their transport in the pores increases the viscosity. As a consequence, the average mobility is reduced. Furthermore, the penetration of solvated ions into the smaller pores may be forbidden. Despite of these considerations, salt polymer interactions favour liquid phase migration inside the greatest pores where no steric hindrance occurs.

(iii) The diffusion coefficients and kinetic absorption constants exhibit an Arrhenius behavior given by the following equations:

$$D = D_0 \exp\left(\frac{-E_{a,D}}{RT}\right) \tag{12}$$

$$k = k_0 \exp\left(\frac{-E_{a,C}}{RT}\right) \tag{13}$$

where $E_{a,D}$ and $E_{a,C}$ are the activation energies of transfer and D_0 as well k_0 are frequency parameters.

Table 2
Thermodynamic parameters deduced from the Arrhenius behaviour of diffusion coefficients D and kinetic absorption constants k reported in Table 1 with temperature (Eqs. (12) and (13))

Liquid phase	D_0 (cm^2 s^{-1})	$E_{a,D}$ (kJ mole^{-1})	k_0 (g cm^{-2} s^{-1})	$E_{a,C}$ (kJ mole^{-1})
Pure VL	0.113	21.8	2.9×10^{-2}	16.2
VL/TFSI (1%)	0.051	20.0	8.0×10^{-3}	13.6
VL/TFSI (12%)	0.513	25.9	0.87	24.2

Table 3
Diffusion coefficients and kinetic absorption constants in relation with the liquid phase composition and silica percentage in the copolymer at 20 °C[a]

Solvent	VL			VL/EC (80/20)		
X_0(SiO$_2$)[b]	0	0.157	0.270	0	0.157	0.270
$m_{l,0}^*$ (mg cm^{-2})[c]	≈ 2	≈ 19	≈ 17	≈ 1.8	≈ 21	≈ 20
$10^5 \times k$ (g cm^{-2} s^{-1})	0.67	3.57	3.72	0.53	3.64	≈ 3.91
$10^5 \times D$ (cm^2 s^{-1})	0.30	1.51	1.40	0.22	1.54	ND[d]

[a] For liquid phases, the salt molar percentage is 8%.
[b] Initial molar fraction of silica in the dry copolymer.
[c] Absorbed weight of liquid phase in the initial stage of superficial wetting of the copolymer by unit surface area of the sample: $m_{l,0}^* = m_{l,0}/S_0$.
[d] Not determined.

The calculated thermodynamical parameters are given in Table 2. A small addition of salt depresses sligthly both $E_{a,D}$ and $E_{a,C}$, but at higher salt content these values are greater than those obtained for the pure solvent. The origin of this observation is probably linked to ion–ion interactions in concentrated organic solutions leading to an increase of energy of the transition state relatively to the initial state in all transport processes described by the Eyring's theory [17].

3.3.2. Influence of solvent composition and silica content in the copolymer at 20 °C

We determine diffusion coefficients and kinetic absorption constants for liquid electrolytes of compositions: pure VL and VL/EC (80/20) with $X_{LiTFSI} = 0.08$. The initial silica contents are: 0, 15.7 and 27% molar percentages in the dry copolymer to obtain final weight percentages, near 4 and 8%, respectively, when silica is present. The results are reported in Table 3. For reasons that will be discussed in the next section, addition of 15.7% SiO$_2$ increases the rate of absorption by a factor 5 (pure VL) or 7 (VL/EC) (see Table 3) but, beyond this limit, this effect seems to be levelled. The solvent composition has no striking influence on the absorption rate.

3.3.3. Absorption ability of the copolymer

The parameters chosen to quantifie the absorption ability of the copolymer are defined in the nomenclature section. A particular attention is devoted to the volumetric fraction of liquid phase at saturation $\Phi_{l,sat}$ which is, as previously stated [18], a predominant factor of gel conductivity. In fact, the conductivity of liquid phase in the gel is calculated by:

$$\sigma_{l,G} = \frac{\sigma_G \Phi_{l,sat}}{100} \tag{14}$$

where

$$\Phi_{l,sat} = 100 \, V_{l,sat} V_{sat}^{-1} \tag{15}$$

with: $V_{l,sat}$ is the volume of liquid phase at saturation in the gel.

Therefore, we determine, for pure VL and VL/LiTFSI solutions at different salt contents wetting PVDF–HFP/SiO$_2$ (73/27) copolymer at four temperatures, $\Phi_{l,sat}$ and the percentage by weight of absorption W_{ab} and by volume V_{ab} which are defined by:

$$W_{ab} = 100 \, m_{l,sat} m_{0,P}^{-1} \quad \text{and} \quad V_{ab} = 100 \, V_{l,sat} V_{0,P}^{-1}$$

where $m_{0,P}$ and $V_{0,P}$ are, respectively, the initial mass and volume of the "dry" copolymer.

The volumic percentages are calculated assuming no compression of the liquid phase in the gel from the experimental determination of absorbed weight and measurement of the volumetric weight of the solutions (see Tables 4 and 5). The results, reported in Table 4 and Fig. 6, clearly show that,

Table 4
Absorption ability of PVDF–HFP/SiO$_2$ (73/27) in relation with the salt molar percentage in the absorbed VL/LiTFSI solutions and with the temperature

%TFSI		0	1	2	4	8	12
V_{ab}[a]		233	187	174	170	140	127
$\Phi_{l,sat}$[a]		89	86.5	83	80	76	68
W_{ab}	0 °C	302	260				177
	10 °C	305	283				181
	20 °C	317	292	264	241	226	202
	30 °C	375	302				220

[a] The liquid volume absorbed is calculated from the weight of absorbed liquid and the volumetric weight determination at 20 °C: $\rho_{liq} = 1.061 + 1.386 \times 10^{-2}$ (%LiTFSI in g cm^{-3}).

Table 5
Absorption ability and conductivity of the resulting gels in relation with the copolymer and solvent compositions[a]

Solvent	VL			VL/EC (80/20)		
$X_0(SiO_2)$[b]	0	0.157	0.270	0	0.157	0.270
$X_G(SiO_2)$[c]	0	0.067	0.113	0	0.065	0.103
$\rho_{0,P}$ (g cm^{-3})[d]	≈1.26	≈0.77	≈0.77	≈1.29	≈0.79	≈0.73
ρ_G (g cm^{-3})[e]	≈1.34	≈1.22	≈1.33	≈1.34	≈1.31	≈1.36
W_{ab}	102	226	220	85	231	203
V_{ab}[f]	110	151	136	87	151	120
$\Phi_{l,sat}$[f]	57	72	76	62	74	75
$m_{l,0}^*$ (mg cm^{-2})	≈3.4	≈19	≈17	≈1.8	≈21	≈20
σ_G (mS cm^{-1})	1.60	2.45	2.42	1.08	2.75	2.35
$\sigma_{l,G}$ (mS cm^{-1})[g]	2.81	3.40	3.18	1.74	3.71	3.13

[a] Initial volumetric weight of the copolymer at 20 °C for the various silica contents. Salt content: $X_{LiTFSI} = 0.08$ in the liquid phase.
[b] Initial molar fraction of silica in the dry copolymer.
[c] Final molar fraction of silica in the saturated gel.
[d] Initial volumetric weight of the dry copolymer.
[e] Final volumetric weight of the gel.
[f] Calculated from volumetric weights at 20 °C: VL/LiTFSI(8%): $\rho = 1.172$ g cm^{-3}; VL/EC(80/20)/LiTFSI(8%): $\rho = 1.214$ g cm^{-3}.
[g] For comparison: liquid electrolytes having the same content in salt at 20 °C: solvent VL: $\sigma = 5.97$ mS cm^{-1}; solvent VL/EC (80/20): $\sigma = 6.97$ mS cm^{-1}.

at a given temperature, the greater the salt content is in the electrolyte, the lower is the final content of liquid phase in the gel (Table 4). At constant composition of liquid phase, an increase of temperature enhances absorption ability of the copolymer (Table 4). A plausible explanation of these experimental results is that ion–polymer interactions may prevent the complete swelling of the material [19]. As temperature rises, the intensity of these interactions decreases leading to an easier expansion of the polymer network.

To complete this study, the determinations of Φ_{ab}, W_{ab} and V_{ab} are made for various silica contents. For this study, the composition of the liquid phase is: solvent VL/EC (80/20) and $X_{LiTFSI} = 0.08$. The results at 20 °C are compared in Table 5. In addition, to clarify the influence of silica, we have
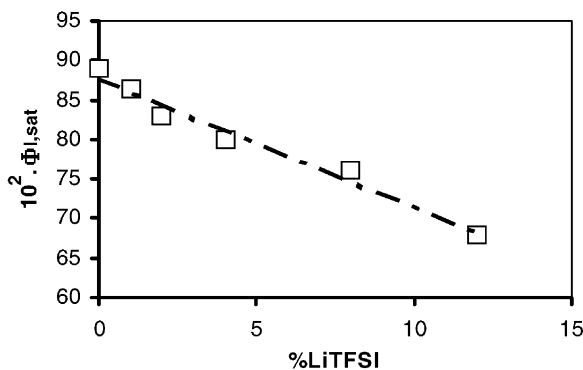

Fig. 6. Volumetric percentage of the liquid phase VL/LiTFSI at saturation in the gel in function of the salt molar percentage in the liquid phase. Copolymer PVDF–HFP/SiO$_2$ (73/27); temperature 20 °C; (□): experimental results; the dotted line is drawn as a guide to the eyes.
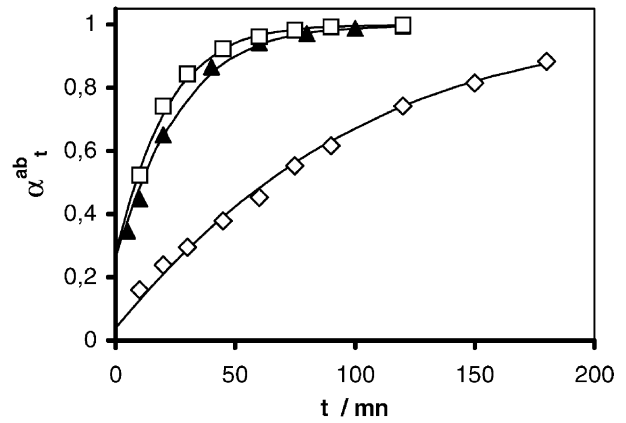

Fig. 7. Evolution of the advancement of absorption α^{ab} with time for copolymers PVDF–HFP of various silica contents at 20 °C. The liquid phase is: VL/LiTFSI (92/8) markers are α_t^{ab} values from experimental determinations of $m_{l,t}$ and $m_{l,sat}$ for the samples;. S$_1$ (◇): $X_0(SiO_2) = 0$; for S$_2$ (▲): $X_0(SiO_2) = 0.157$ for S$_3$ (□): $X_0(SiO_2) = 0.270$.

reported the initial volumetric weights of copolymers and final volumetric weights of the gels with the conductivities of gels and liquid phase in the gels (Eq. (14)). We also calculate the initial adsorbed weight of liquid phase by unit surface area of the samples. As for kinetics constants, the nature of the solvent has little influence on absorption ability. The most important parameter is the initial volumetric weight which is directly related to the porosity of the copolymer. The addition of silica increases the absorption speed and ability because it increases the porosity. When maximum porosity is reached, further addition decreases absorption ability and conductivity by restricting the porous volume (silica itself is not a porous material) and by fixation of some fraction of the lithium salt [7].

To make clear the great importance of silica addition to polymer to permit comparison of results, it is useful to calculate the advancement of the process at different times, α_t^{ab}, as presented in Fig. 7 for the absorption of VL/LiTFSI (92/8) solution at 20 °C in copolymer of initial molar fractions in SiO$_2$: $X_0(SiO_2) = 0$, 0.157 and 0.270. The curves drawn on Fig. 7 are calculated from $m_{l,t}$ evolution and parameters reported below:

Sample	S$_1$	S$_2$	S$_3$
S_0 (cm^2)	2.800	2.836	2.793
S_{sat} (cm^2)	3.856	4.354	4.187
$m_{l,0}$ (mg)	46	54	48
$m_{l,sat}$ (mg)	120	206	170
$10^2 k_{exp}$(mn^{-1})	1.29	4.53	5.50

As we can see, simulated evolution fits well experimental values of α_t^{ab}. Silica enhances the initial "superficial" absorption and makes faster the copolymer saturation. There is no real difference when initial silica content is raised from $X_0(SiO_2) = 0.157$ to $X_0(SiO_2) = 0.270$. We focus our attention on the time required to obtain α_t^{ab} values, respectively,

Table 6
Time (in minutes) of polymer–liquid solution contact required for various advancement of absorption at 20 °C[a]

X_0 (SiO$_2$)[b]	0	0.157	0.270
$\alpha^{ab} = 0.50$	63	12	8.25
$\alpha^{ab} = 0.95$	252	67	53
$\alpha^{ab} = 0.99$	376	102	83

[a] The liquid solution is VL/LiTFSI (92/8).
[b] Initial molar fraction of silica in the dry copolymer.

equal to 0.5, 0.95 and 0.99. Results are given in Table 6 and we can conclude that, if 95% of maximum absorption is achieved providing adequate conductivity for industrial applications, it is not necessary to reach saturation of the copolymer which require a much longer time of wetting.

4. Conclusion

The absorption kinetics and absorption ability of a PVDF–HFP copolymer toward VL/LiTFSI and VL/EC/LiTFSI electrolytes has been studied. The effect of silica addition to the copolymer has also been investigated. Some important features for this method of gel-electrolyte synthesis have been revealed:

(i) In addition to provide better mechanical properties to the conducting membrane, silica increases the porosity of the dry copolymers. Consequently, the volume of the liquid phase in the gel becomes higher and the conductivity increases. This effect is levelled off by the fixation of a fraction of salt on silica, and an addition of 15% (in moles) in the PVDF–HFP copolymer leads to the highest conductivity by incorporation of liquid electrolytes with a salt molar percentage of about 8%. The faster wetting observed in the presence of silica is an other advantage for industrial purpose: the time required for saturation by the liquid electrolyte is reduced four times at 20 °C.

(ii) Any increase in salt content in the liquid electrolyte leads to a lower absorption ability by the copolymer. This behaviour is related to bonding interactions between ions and polymer chains. As a result, the maximum conductivities for the liquid electrolyte and for the gel are not correlated.

(iii) Finally, increasing the temperature of wetting increases both the rate and ability of absorption. The temperature of liquid electrolyte absorption can be raised advantageously within the limits of thermal stability of the components. As a matter of fact, this is an irreversible process, meaning that, on cooling back to ambient temperature, the gel will not lose some fraction of the retained liquid electrolyte. Actual work is in progress to test the thermal stability of gels prepared by differential scanning calorimetry and thermogravimetry.

References

[1] M. Watanabe, M. Kanba, H. Matsuda, K. Mizogushi, I. Shinoshara, E. Tscuchida, K. Tsunemi, Makromol. Chem. Rapid. Commun. 2 (1981) 741.
[2] A.S. Godz, C.N. Schmutz, J.M. Tarascon, US Patent No 5,296,318, (1994).
[3] J.M. Tarascon, A.S. Godz, C.N. Schmutz, F. Shukoki, P.C. Warren, Solid State Ionics 49 (1996) 86.
[4] J.Y. Song, Y.Y. Wang, C.C. Wan, J. Power Sources 77 (1999) 183.
[5] J.Y. Song, Y.Y. Wang, C.C. Wan, J. Electrochem. Soc. 147 (2000) 3219.
[6] K.M. Abraham, Electrochemica Acta 38 (1993) 1233.
[7] K.H. Lee, Y.G. Lee, J.-Y. Park, D.-Y. Seung, Solid State Ionics 133 (2000) 257.
[8] R. Jasinski, Electrochem. Technol 6 (1968) 28.
[9] B.E. Blomgren, Lithium Batteries, Academic Press, New York, 1983.
[10] Z. Ziang, B. Caroll, K.M. Abraham, Electrochemica. Acta 42 (1997) 2667.
[11] A. Webber, J. Electrochem. Soc. 138 (1991) 2586.
[12] S. Iylla, J.Y. Sanchez, M. Armand, Electrochim. Acta 37 (1992) 1699.
[13] A. Ferry, M.M. Doeff, L.C. de Jonghe, J. Electrochem. Soc. 145 (1998) 1586.
[14] I. Rey, J.L. Bruneel, J. Grondin, L. Servant, J.C. Lassegues, J. Electrochem. Soc. 145 (1998) 3034.
[15] J. Crank, G.S. Park, Diffusion in Polymers Chains, Academic Press, 1968 (chapter 8).
[16] J. Crank, The Mathematics of Diffusion, 2nd Edition, Oxford University Press, 1975.
[17] J.F. Kincaid, H. Eyring, Chem. Rev. 28, 1941.
[18] M. Caillon-Caravanier, B. Claude-Montigny, D. Lemordant, G. Bosser, Solid State Ionics, submitted for publication.
[19] F.M. Gray, Solid Polymer Electrolytes, VCH Publishers Inc., Cambridge, 1991.